DOI: 10.21062/mft.2024.098 http://www.journalmt.com

The Influence of the Crane Track Unevenness on the Load of the Supporting Crane Structure

Ján Vavro (0009-0009-6787-9041), Ján Vavro jr. (0009-0001-3704-4934), Ľuboš Marček (0009-0005-3699-0100)[1], Jana Kuricová (0009-0005-4560-884X), Miloš Taraba (0009-0000-2006-8350), Lukáš Klimek (0009-0000-9525-414X), Pavol Čerňava (0009-0006-5455-6305)
Faculty of Industrial Technologies in Púchov, Alexander Dubček University of Trenčín, I. Krasku 491/30, 020 01 Púchov, Slovakia. E-mail: jan.vavro@tnuni.sk, jan.vavro.jr @tnuni.sk, lubos.marcek@tnuni.sk, milos.taraba@tnuni.sk, jana.kuricová@tnuni.sk, lukas.klimek@tnuni.sk, pavol.cernava@tnuni.sk

The paper presents the analysis of the gantry crane loading when driving along the crane track, using a 3D model, for which the analysis of the gantry crane frame loading was performed. The gantry crane is designed to remove dirt that is in front of the turbine under the water surface. For the gantry crane which moves along a track, the directional and vertical unevennesses were determined by experiment and are given in graphic and numerical form in (mm), relating to A track and B track with a total track length of 450 (m). Based on the knowledge of the unevenness of the rail track, the four random functional dependencies defining the irregularities of the individual rails as input variables were used for the kinematic excitation of the individual wheels of the gantry crane. The stress analysis was performed for a travel speed of 30 (m.min^{-1}) and a lift of 10 (t) under the given loading. The results of the stress analysis are presented in graphic form.

Keywords: Loading, virtual model, load, stress analyse, 3D model

1 Introduction

The solution of the real practice problems often involves solving the complex systems, including differential, integral as well as algebraic equations. In the most cases, it is impossible to obtain analytical solutions and therefore, the designers utilise the specialised numerical processing methods with the use of modern computational technology.

Modern computational methods depend on the creation of a virtual model with subsequent simulation of the operating process of a given system without which the work of the designer is unthinkable and impossible in relation to solving the complex problems, the solution of which often brings the significant economic benefits.

Based on the requirements of the practice, the main task of designer is to design and modify the parameters of the proposed device appropriately and precisely, taking into account the other important and specific features of device, such as its mass, shape, geometry, or some other dynamic properties. The main objective is usually to be able to save material and to find the best solution in terms of material utilization and suitable shape of the structure.

Nowadays, the increased requirements for material saving, durability, reliability of products and machinery require some new approaches in solving the challenges of the engineering practice. With the help of the adequate and suitable computational programs a precise, quick and efficient study can be made because in more or less extend, this study can be important material from the aspect of the influence of the static and dynamic characteristics of the machine.

2 Crane rail track measurement results (directional and vertical deflections)

Track unevenness or irregularities are usually divided into vertical (height) and directional (transverse). The above-mentioned track unevenness results in excitation for the vertical movement of the (vehicle) – vertical unevenness or irregularities and transverse elevation of the track rails usually in the form of angular shifts (this represents one of the excitation inputs for the transverse travel of the vehicle). In relation to the transverse unevenness or irregularities, the crosswise deflections of the track centreline and the rail gauge deflection are usually considered. This means that the four excitation random functions (left and right rail in both transverse and vertical directions) result into four, which are related to certain types of oscillatory motion of the gantry crane (vehicle).

The rail track is a complex dynamic system that changes its shape when it is subjected to variable movement loads which are caused by the double wheels of the rail cranes (vehicles). The change in the shape of the track is random because its flexure is influenced by the following factors:

- the vertical flexuosity of the rails,
- the elastic pads between the rail flange and the foundation,
- the quality of the ballast bed, especially the condition how the individual sleepers are fastened,
- defects in the load-bearing capacity of the railway construction (structure),
- the dynamic characteristics of the rail crane (vehicle) which moves on the rail.

In this case, since the rail track is embedded in concrete, the dynamic properties of the gantry crane (vehicle) are going to be only considered.

The experimental investigation of the rail unevenness or irregularities is based on geodetic methods. The measurement of the vertical and transversal unevenness of the rails was for the purpose of defining the kinematic excitation of the gantry crane moving along the track. The measurement was made using a digital theodolite with a Leica laser. The irregularities of the track were measured in whole millimeters. The stochastic character of the excitation was modeled on the basic of the vertical and transversal track unevenness obtained from the measuring on real track and the course of the random kinematic excitation functions is shown in the Fig. 1 and the Fig. 2.

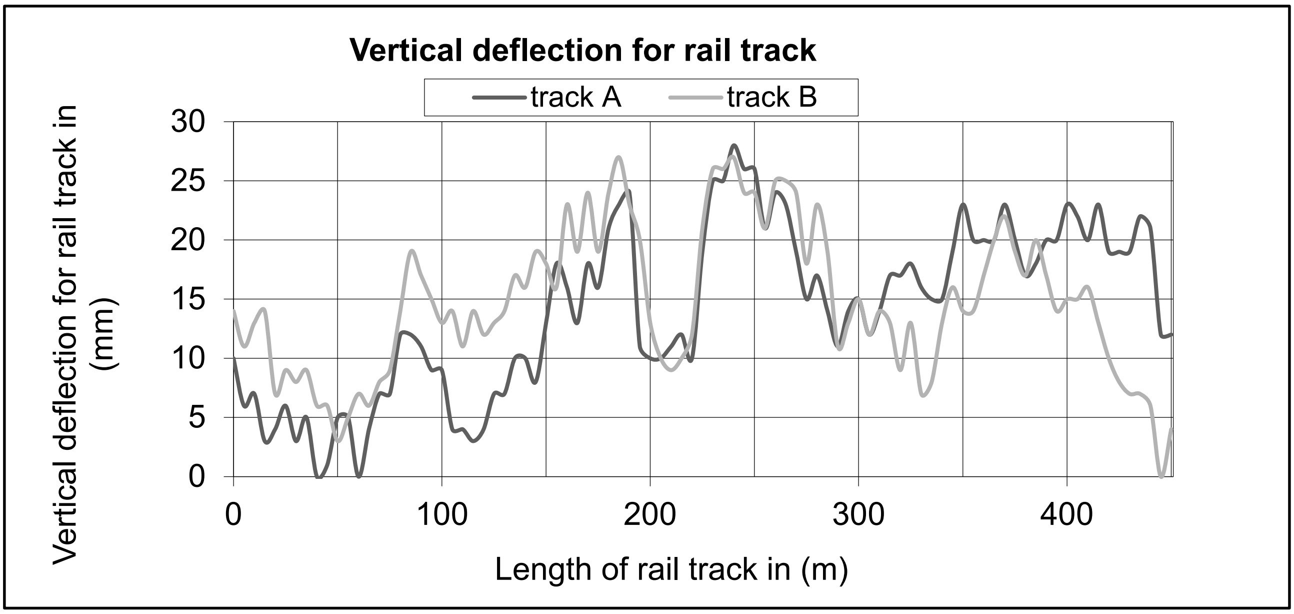

***Fig. 1** The vertical deflections – the unevenness (irregularities) for the rails –* $u_{yL}^{(1)}$ *(rail designated as A) and* $u_{yP}^{(1)}$ *(rail designated as B)*

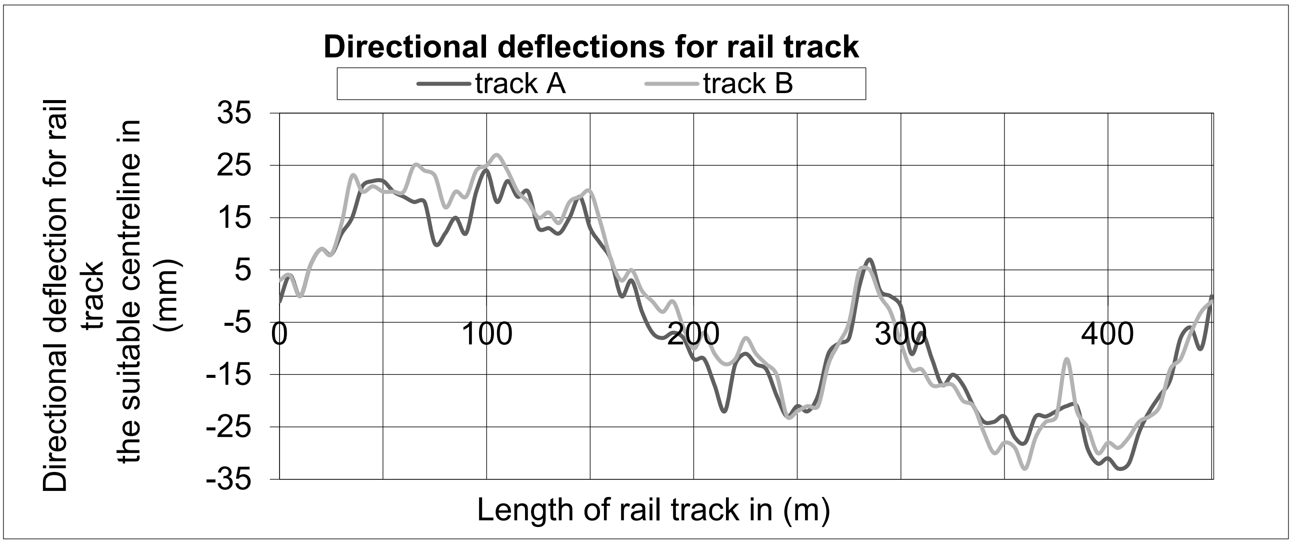

***Fig. 2** The directional deflection – the unevenness (irregularities) for the rails –* $u_{xL}^{(1)}$ *(rail designated as A) and* $u_{xP}^{(1)}$ *(rail designated as B)*

The numerical values of deflections for the rail track vertical (height) unevenness (irregularities) are shown in Tab. 1 and the numerical values of deflections for the rail track directional (transverse) unevenness (irregularities) are given in Tab. 2.

Tab. 1 *The values of deflections for the rail track vertical (height) unevenness (irregularities)*

No.	Length of rail track (m)	Rail designated as A (mm)	Rail designated as B (mm)	No.	Length of rail track (m)	Rail designated as A (mm)	Rail designated as B (mm)
1	0	10	14	47	230	25	26
2	5	6	11	48	235	25	26
3	10	7	13	49	240	28	27
4	15	3	14	50	245	26	24
5	20	4	7	51	250	26	24
6	25	6	9	52	255	21	21
7	30	3	8	53	260	24	25
8	35	5	9	54	265	23	25
9	40	0	6	55	270	19	24
10	45	1	6	56	275	15	18
11	50	5	3	57	280	17	23
12	55	5	5	58	285	14	19
13	60	0	7	59	290	11	11
14	65	4	6	60	295	14	13
15	70	7	8	61	300	15	15
16	75	7	9	62	305	12	12
17	80	12	14	63	310	14	14
18	85	12	19	64	315	17	13
19	90	11	17	65	320	17	9
20	95	9	15	66	325	18	13
21	100	9	13	67	330	16	7
22	105	4	14	68	335	15	8
23	110	4	11	69	340	15	13
24	115	3	14	70	345	19	16
25	120	4	12	71	350	23	14
26	125	7	13	72	355	20	14
27	130	7	14	73	360	20	17
28	135	10	17	74	365	20	20
29	140	10	16	75	370	23	22
30	145	8	19	76	375	20	19
31	150	13	18	77	380	17	17
32	155	18	16	78	385	18	20
33	160	16	23	79	390	20	17
34	165	13	19	80	395	20	14
35	170	18	24	81	400	23	15
36	175	16	19	82	405	22	15
37	180	21	24	83	410	20	16
38	185	23	27	84	415	23	13
39	190	24	23	85	420	19	10
40	195	11	20	86	425	19	8
41	200	10	13	87	430	19	7
42	205	10	10	88	435	22	7
43	210	11	9	89	440	21	6
44	215	12	10	90	445	12	0
45	220	10	12	91	450	12	4
46	225	19	21				

ISSN 1213–2489
e-ISSN 2787–9402

Tab. 2 *Values of deflections for the rail track directional (transverse) unevenness (irregularities)*

No.	Length of rail track (m)	Rail designated as A (mm)	Rail designated as B (mm)	No.	Length of rail track (m)	Rail designated as A (mm)	Rail designated as B (mm)
1	0	-1	3	47	230	-13	-11
2	5	4	4	48	235	-14	-13
3	10	0	0	49	240	-19	-15
4	15	6	6	50	245	-23	-23
5	20	9	9	51	250	-21	-22
6	25	8	8	52	255	-22	-21
7	30	12	14	53	260	-19	-21
8	35	15	23	54	265	-11	-13
9	40	21	20	55	270	-9	-9
10	45	22	21	56	275	-8	-5
11	50	22	20	57	280	2	5
12	55	20	20	58	285	7	5
13	60	19	20	59	290	1	0
14	65	18	25	60	295	0	-3
15	70	18	24	61	300	-2	-9
16	75	10	23	62	305	-11	-14
17	80	12	17	63	310	-7	-14
18	85	15	20	64	315	-12	-17
19	90	12	19	65	320	-17	-17
20	95	20	24	66	325	-15	-17
21	100	24	25	67	330	-17	-20
22	105	18	27	68	335	-21	-21
23	110	22	24	69	340	-24	-26
24	115	19	20	70	345	-24	-30
25	120	20	18	71	350	-23	-28
26	125	13	15	72	355	-27	-29
27	130	13	16	73	360	-28	-33
28	135	12	14	74	365	-23	-27
29	140	15	18	75	370	-23	-24
30	145	19	19	76	375	-22	-23
31	150	13	20	77	380	-21	-12
32	155	10	14	78	385	-21	-22
33	160	7	7	79	390	-29	-25
34	165	0	3	80	395	-32	-30
35	170	3	5	81	400	-31	-28
36	175	-3	1	82	405	-33	-29
37	180	-7	-1	83	410	-32	-27
38	185	-8	-3	84	415	-26	-24
39	190	-7	-1	85	420	-22	-23
40	195	-8	-6	86	425	-19	-21
41	200	-12	-10	87	430	-16	-14
42	205	-12	-7	88	435	-8	-12
43	210	-17	-11	89	440	-6	-7
44	215	-22	-13	90	445	-10	-3
45	220	-13	-12	91	450	0	-1
46	225	-11	-8				

3 Computer verification of the crane computational model

The gantry crane (Fig.3) is designed to remove debris (waste) that is below the water surface in front of the turbine. The gantry crane was made of plain carbon structural steel and according to Slovak technical standards (STN), the designation of this steel is 10 373 and in present, the equivalent of the given steel is 11 373 (EN ISO S235JRG1 = 1.0036). The crane construction steel is susceptible to ageing.

The required mechanical properties of the given steel are:

- $R_{e\ min}$=235 [MPa] (yield point),
- R_m=340-470 [MPa] (tensile strength),
- σ_{all} = 210 [MPa] (allowable stress).

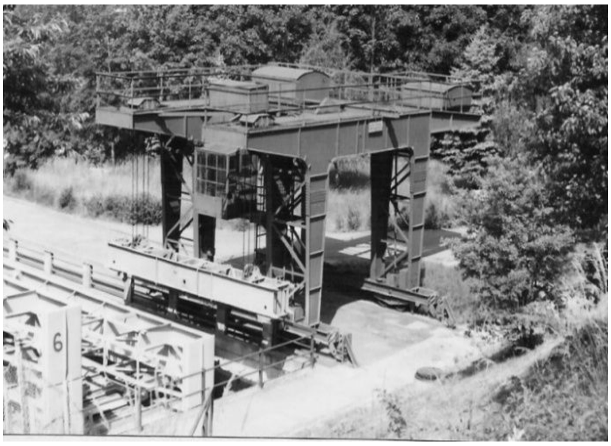

Fig. 3 *The view of the portal gantry crane*

The operating mode of the gantry crane (operating cycle) can be described in these steps:

- movement (travelling) of the crane along the track at the specified degree of travelling speed without any load,
- lifting of the load,
- movement of the crane along the track at the specified travelling speed with load.

The following parameters are used as input parameters for the computational model:

- Young's modulus of elasticity: E=210 [GPa],
- Poisson's number: μ=0.3,
- the density of the material: ρ=7800 [kg.m^{-3}].

External loading:

- load to be lifted: Q =32 [t], 10 [t], 5 [t],
- weight of the crane and individual aggregates according to the technical documentation (drawings),
- kinematic excitation resulting from unevenness of the rail track.

On the basis of the known unevenness (irregularities) of the rail track, four random functional dependencies (Fig. 1 and Fig. 2), which define the unevenness of individual rails in dependency on the track, are used as input variables for the kinematic excitation of the individual wheels of the gantry crane [1-4].

Where:

v…Gantry crane speed: v = 30 (m.min^{-1}),

L…Wheel base 5.2 (m),

$u_{xL}^{(1)}$ …Unevenness of the left rail in transverse direction for the front axle,

$u_{yL}^{(1)}$ …Unevenness of the left rail in vertical direction for the front axle,

$u_{xP}^{(1)}$ …Unevenness of the right rail in transverse direction for the front axle,

$u_{yP}^{(1)}$ …Unevenness of the right rail in vertical direction for the front axle,

$u_{xL}^{(2)}$ …Unevenness of the left rail in transverse direction for the rear axle, i.e. $u_{xL}^{(2)}(t) = u_{xL}^{(1)}\left(t - \frac{L}{v}\right)$,

$u_{yL}^{(2)}$ …Unevenness of the left rail in vertical direction for the rear axle, i.e. $u_{yL}^{(2)}(t) = u_{yL}^{(1)}\left(t - \frac{L}{v}\right)$,

$u_{xP}^{(2)}$ …Unevenness of the right rail in transverse direction for the rear axle, i.e. $u_{xP}^{(2)}(t) = u_{xP}^{(1)}\left(t - \frac{L}{v}\right)$,

$u_{yP}^{(2)}$ …Unevenness of the right rail in vertical direction for the rear axle, i.e. $u_{yP}^{(2)}(t) = u_{yP}^{(1)}\left(t - \frac{L}{v}\right)$.

In reference to the technical documentation (drawing), a finite element model of the gantry crane construction (structure) was created in 3D MODEL (Fig. 4 and Fig. 5) for which the analysis of the loading for gantry crane frame, resulting from the operating loading, modal analysis and crane stability loss was performed [5-9].

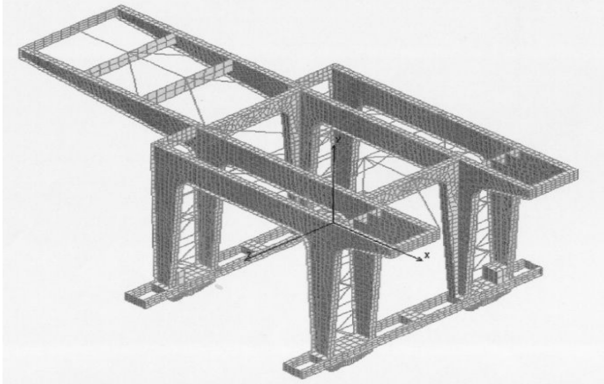

Fig. 4 *The finite element model of the gantry crane frame*

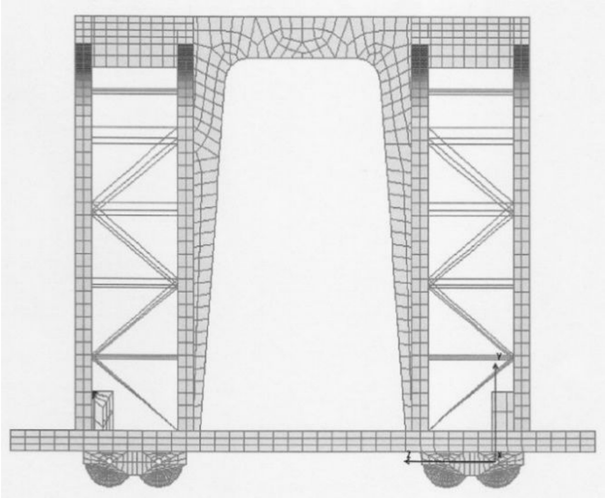

Fig. 5 *The view of the finite element model in the direction of x-axis*

4 Results for loading and stability loss for gantry crane supporting construction (frame)

In the Fig. 6, there is the stress (loading) distribution for the crane construction with the respect to the loading relating to the own crane weight and the weight of the individual aggregates (according to technical drawings), the lifted load of 10 [t] and the travelling speed of 30 [m.min^{-1}]. This is the maximum value of stress that is allowed to be reached during the operating process of gantry crane. The specified value of stress for the construction is not going to be beyond the yield stress (σ_{all}) = 210 [MPa] and in relation to calculated stress ($\sigma_{cal.}$), the loading condition can be expressed as $\sigma_{all} \geq \sigma_{cal.}$.

In the case of investigated loading for gantry crane, the value of 210 [MPa] is higher than calculated value, which was 185.69 [MPa] and it means that the gantry crane construction is suitable for the loading during the operating process of crane. The magnitude of the load is affected by the vertical (height) and directional (transverse) deflections of the track.

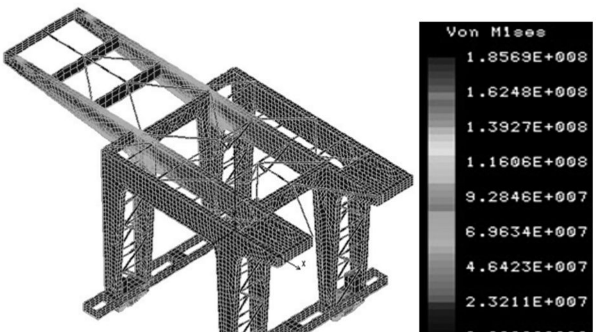

Fig. 6 *The maximum stress distribution in track point of 100 [m] and lift of 10 (t) in [Pa]*

In the Fig. 7, there is the maximum stress distribution in track point of 250 [m] for the gantry crane supporting construction (frame) and for a lift of 10 [t] at travelling speed of 30 [m/min].

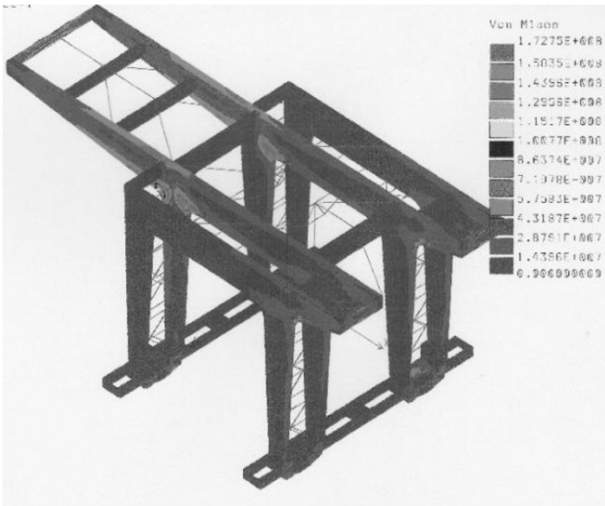

Fig. 7 *The maximum stress distribution in track point of 250 [m] and lift of 10 (t) in [Pa]*

In the Fig. 8, there is the stress (loading) distribution for the crane supporting construction (frame) with the respect to the loading relating to the own crane weight and the weight of the individual aggregates (according to technical drawings) for the lifted load of 32 [t] and the specified travelling speed on the rail track. This is the minimum value of stress that is reached during the operating process of gantry crane. The specified value of stress for the construction was not beyond the yield stress (σ_{all}) = 210 [MPa] and in relation to calculated stress ($\sigma_{cal.}$), the loading condition can be expressed as $\sigma_{all} \geq \sigma_{cal.}$.

Relating to this case, there is: 210 [MPa] is ≥142.3 [MPa] and it means that the gantry crane support konstruction is suitable for the given load of crane operation. The magnitude of the load is influenced by the vertical (height) and directional (transverse) deflections of the track.

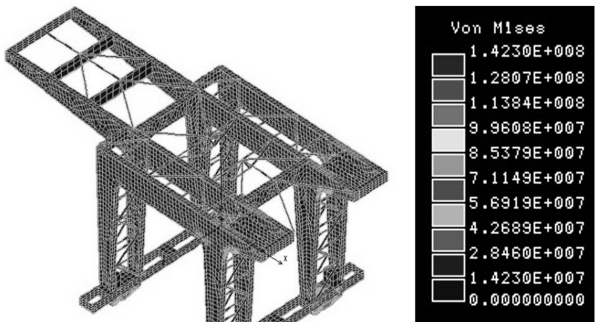

Fig. 8 *The minimum stress distribution for lift of 32 (t) in [Pa]*

The stability of the crane (Fig. 9) was performed for a lifted load of 10 [t], a crane travelling speed of 30 [m/min] and for specified unevenness of the rail track in the vertical and transverse direction at a point in the track of 250 [m].

An overall loss of stability occurs when an overloading force of 16 839 [N] is applied when the travelling wheel loses contact with the rail. For the loading, (see Fig. 7), the overall loss of the stability can occur at an overloading force of 11764 [N] during the loss of contact of the travelling wheel with the rail.

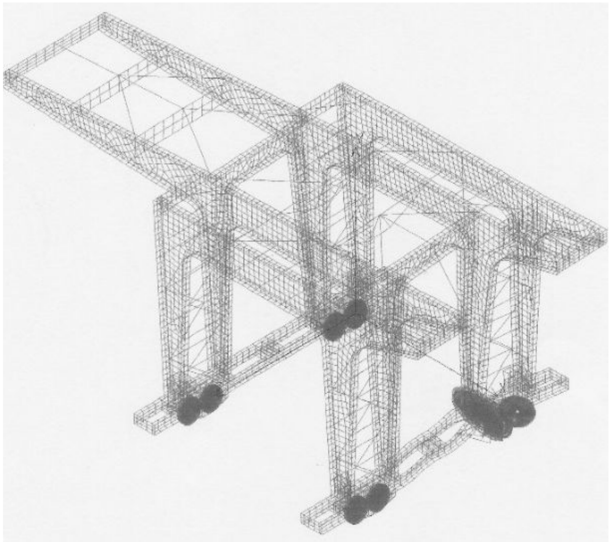

Fig. 9 *The global loss of crane stability in track point of 100 [m] and lift of 10 (t)*

5 Conclusion

The reliable and safe operating process of a gantry crane depends on several factors. The loading represents one of the main factors which have to be taken into account in relation to the reliability of the gantry crane. The given loading is not allowed to exceed a certain value of the allowable load on the construction when it is in operating mode. The given loading condition is expressed in the form of $\sigma_{all} \geq \sigma_{cal.}$, where σ_{all} represents the allowable stress of a given material and $\sigma_{cal.}$ is the calculated stress for the construction in relation to a given specific load.

The gantry crane loading ranges from 142.3 [Mpa] to 185.69 [MPa]. The gantry crane supporting construction (frame) is suitable for the reliable operation of the given crane. The maximum load of 185.69 [MPa] is less than thealoweable load of 210 [MPa]. The measure of the load is also affected by the vertical (height) and directional (transverse) deflections of the rail track.

The stability is the second important factor in relation to the gantry crane during operating process. The given stability is closely related to the load on the crane structure. The loss of stability is possible in the case if the external load was increased by the critical force ($F_{crit.}$) = 0.039701. In the Fig. 6, the external force ($F_{ext.}$) is 0.039701*296318=11764 [N] for track point of 100 [m] and lift of 10 [t]. The stability of the crane depends on the external loading as well as on the unevenness of the rail track. In the case of 172 [MPa] loading (Fig. 7), there is the loss of stability when the value of $F_{crit.}$ is exceeded (see: $F_{crit.}$ = 0.0455111*$F_{ext.}$ = 0.455111*370000 = 16839 [N]).

The measure of stability can be increased significantly if the travelling speed is limited to 15 [m.min^{-1}] and if two different operating activities are not performed simultaneously, i.e. lifting and travelling at the same time. The stability of gantry crane is also based on the eigenfrequency (natural frequency) of the crane. The modal analysis shows that the first eigenfrequency (natural frequency) of the crane has the most significant or the greatest effect.

Acknowledgement

This work was supported by the Slovak Grant Agency – project KEGA 011TnUAD-4/2024.

References

[1] BRÁT, V., (1976), *Handbook of Kinematics with Examples*, Prague, SNTL

[2] DIŽO, J., HARUŠINEC, J., BLATNICKÝ, M. (2018). Computation of modal properties of two types of freight wagon bogie frames using the finite element method. In: *Manufacturing Technology*. Vol. 18, No. 2, pp. 208–214. J. E. Purkyne University in Usti n. Labem. Czech Republic

[3] GERLICI, J., GORBUNOV, M., KRAVCHENKO, K., DOMIN, R., LACK, T. (2017) Slipping and Skidding Occurrence Probability Decreasing by Means of the Friction Controlling in the Wheel-Braking Pad and Wheel-Rail Contacts. In.: *Manufacturing Technology*. Vol. 17, No.2, pp. 179-186, ISSN 1213-2489

[4] HAUSER, V., NOZHENKO, O. S., KRAVCHENKO, K. O., LOULOVÁ, M., GERLICI, J., LACK, T. (2017). Impact of Wheelset Steering and Wheel Profile Geometry to the Vehicle Behavior when Passing Curved Track. In.: *Manufacturing Technology*. ISSN 1213-2489 vol. 17, pp 306-312

[5] KLIMENDA, F., SOUKUP, J., SKOČILASOVÁ, B., SKOČILAS, J. (2020). Vertical Vibration of the Vehicle when Crossing over Transverse Speed Bumps. DOI: 10.21062/mft.2020.020 © *Manufacturing Technology*. Vol. 20, No. 1 ISSN 1213–2489

[6] SAGA, M., VAVRO, J., KOPECKÝ, M., (2002), *Počítačová analýza a syntéza mechanických sústav*. ISBN 80-968605-4-2, Žilina, 267 s.

[7] SVOBODA, M., CHALUPA, M., ČERNOHLÁVEK, V., ŠVÁSTA, A., MELLER, A., SCHMID, V. (2023). Measuring the Quality of Driving Characteristics of a Passenger Car with Passive Shock Absorbers. In.: *Manufacturing Technology*. Vol. 23, No. 1 ISSN 1213–2489 e-ISSN 2787–9402, DOI: 10.21062/mft.2023.023 © 2023

[8] TOMSOVSKY, L., LOPOT, F., JELEN, K. (2022). Kinematic Analysis of the Tram-pedestrian Collision - a Preliminary Case Study. In.: *Manufacturing Technology*. Vol. 22, No. 1 ISSN 1213–2489, DOI: 10.21062/mft.2022.007 © 2022

[9] VAVRO, J., (2020), *Kinematic and Dynamic Analysis of Planar Mechanisms by Means of the SolidWorks Software*, Tribun EU s. r. o., ISBN 978-80-263-1495-0, p. 156.